PHYSICAL REVIEW B **82**, 094443 (2010)

Effect of metallic surfaces on the electronic structure, magnetism, and transport properties of Co-phthalocyanine molecules

Xi Chen and M. Alouani
Institut de Physique et de Chimie des Matériaux de Strasbourg (IPCMS), UMR 7504, UdS–CNRS, 23 rue du Loess, 67034 Strasbourg, France, EU

(Received 13 April 2010; revised manuscript received 23 July 2010; published 28 September 2010)

The effects of ferromagnetic Co(111) and paramagnetic Cu(111) substrates on the electronic and magnetic structures of Co-phthalocyanine (CoPc) molecule were systemically investigated by means of a plane-wave ultrasoft pseudopotential *ab initio* electronic-structure calculations within both the local-density approximation and generalized gradient approximation including van der Waals interaction within the Grimme approximation. A strong chemisorption of the CoPc molecule on the Co(111) substrate and a weaker one on the Cu(111) substrate have been found and explained in terms of charge transfer at the interface and the strength of the hybridization between the molecular orbitals and the substrate states. These combined effects at the interface reduce drastically the magnetic moment of CoPc on Co(111) and suppress it for CoPc on Cu(111). It is also found that the calculated scanning tunneling spectroscopy (STM) images at the vicinity of the Fermi level agree qualitatively with experiment, and the STM magnetoresistance occurs only when the CoPc molecule is deposited on Co substrate and is in qualitative agreement with recent experimental results.

DOI: 10.1103/PhysRevB.82.094443 PACS number(s): 71.20.−b, 71.15.Pd, 72.25.Mk

I. INTRODUCTION

The miniaturization of electronic devices based on semiconductor industry has always followed Moore's law. However, the physical limit will be reached in the near future. New concepts are therefore required to continue the downscaling of electronic and magnetic devices. The burgeoning field of molecular electronics offers a natural continuation in spintronics physics at the nanoscale since it is today possible to manipulate and control the electron spin at the molecular level.[1–4] To make progress in this new field, it is important to choose a suitable functional molecule for making molecular junctions. The family of phthalocyanine (Pc) offers a potential choice for this purpose because of their thermal stability and the possibility to tune their structure, chemical, magnetic, and transport properties by means of different metallic cations within the Pc molecular cage or by moving some atoms in the lobes.

The most important characteristics of a molecular junction are the electron transfer rates between the molecule and metallic electrodes as well as its magnetic state. In particular, metallic substrates have a strong effects on the electronic, magnetic, and transport properties of molecules. Indeed a recent experimental work[5] shows that the CoPc molecule, deposited on magnetic cobalt or paramagnetic copper surfaces, behaves differently, i.e., the interaction between the molecule and the Co substrate is much stronger than that with the Cu substrate. The hybridization of the molecular orbitals with the substrate states and their energy shift have also been determined by scanning tunneling spectroscopy[5] (STM).

From the theoretical point of view, it is difficult to investigate the interaction of a complex molecule, such as phthalocyanine, with a substrate without performing a state of the art *ab initio* calculation of its electronic structure. In order to compute the interaction of the molecule with the substrate, it is important to carry out an atomic relaxation of the whole system, allowing thus the molecule to adjust to the surface by letting its localized orbitals hybridize with the continuum states of the substrate. In the last few years, different studies of the physics of the Pc molecule have been conducted,[5–12] such as the controllable Kondo effect,[6–8] the manipulation of a single spin of CoPc molecule,[6,9] as well as the quantum transport through CoPc molecule junction.[5,9–11] Most of the calculations are done within a simple model[7,8] and do not capture the subtlety of the chemical bonding which is crucial for a detailed analysis of the interaction of the localized molecular orbitals with the continuum states of the substrate.

The aim of the present work is to use an *ab initio* method to calculate the interaction of a CoPc molecule with metallic surfaces in order to systematically investigate the substrate effects on the physics of molecular junctions based on CoPc molecule and to explain the recent STM results.[5,9] Our study of both Co(111) and Cu(111) substrates shows that the hybridization of the molecular orbitals with the substrate states and the rearrangement of the electron density at the interface depend strongly on the filling of the d states of the substrate. For Co(111), where the Co $3d$ states are partially filled, the CoPc molecule is strongly chemisorbed and the substrate Co $3d$ projected density of states (PDOS) exhibits a substantial energy overlap with those of CoPc, whereas it is only weakly chemisorbed when the $3d$ states are completely filled like in the case of Cu(111) substrate. We have also shown that the charge transfer from the substrate to the molecule reduces strongly the magnetic moment of CoPc molecule. When CoPc is adsorbed on Cu(111) the Co atom loses completely its magnetic moment and when it is adsorbed on Co(111) it is strongly reduced despite the strong magnetic field emanating from the Co substrate. This strong reduction in the Co magnetic moment is due to the substrate $4s$ electrons magnetic screening of the spin of Co in CoPc similar to a Kondo-type physics. To understand further this effect we have studied the magnetic state of CoPc molecule when it is approaching the Co or Cu substrate and showed how it

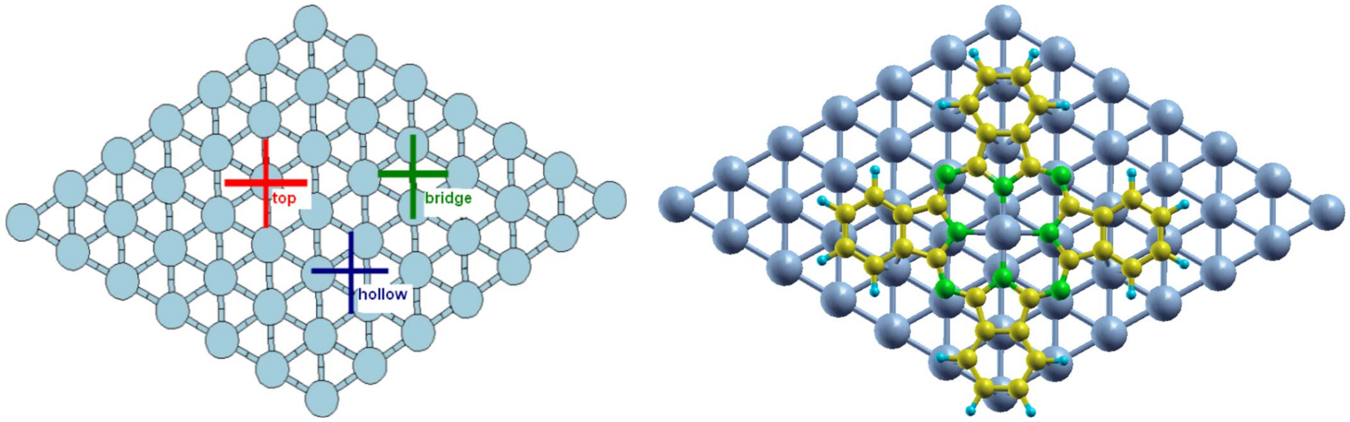

FIG. 1. (Color online) The left figure shows the high-symmetry sites of Co(Cu) (111) surface and the right figure the position of the CoPc molecule centered on the bridge position.

evolves as a function of the molecule-substrate distance. To study the transport properties of CoPc we have first calculated STM images with the Tersoff-Hamann approximation[13] and compared them to experiment, and used a Bardeen approximation[14] for the calculation of the current versus the bias voltage. Our calculation shows that an STM magnetoresistance is possible only in the case of CoPc on Co(111).

Our manuscript is organized as follows. In Sec. II we describe briefly our method of calculation. In Sec. III we present our results concerning adsorption energy of a CoPc molecule on Co(111) or Cu(111). We discuss first the stability of the CoPc molecule and its electronic and magnetic properties within local-density approximation (LDA) and generalized gradient approximation plus van der Waals (GGA+vdW). Then we show how the charge transfer and the electric dipole at the interface modify the magnetic properties of the molecule. Finally, well show our calculation of STM images and the STM spin-dependent electric conductance.

II. METHOD OF CALCULATION

Our study is based on *ab initio* ultrasoft pseudopotential calculations and uses the PWSCF package.[15,16] The LDA (Ref. 17) and GGA (Ref. 18) ultrasoft pseudopotentials as provided by the QUANTUM ESPRESSO website[19,20] have been used. The exchange and correlation potentials are within the Kohn-Sham LDA as parametrized by Perdew and Zunger[21] or the GGA+vdW interaction within the Grimme approximation.[22] The substrates are modeled by a slab consisting of five layers. For the Co substrate we used two layers of hcp Co on top of three layers of Cu(111) while for the Cu substrate we used five layers of Cu(111). In both cases, we used 302 atoms in the supercell and more than 2 nm vacuum to the next periodic repeated slab. We should emphasis that 5 monolayers are enough for the convergence of the total energy and density of states. We have showed that a 3 monolayers and 7×7 or 10×10 supercells produced very similar DOS, and also that 3 and 5 monolayer supercells produced adsorption energies and DOS that are not significantly different from each others. We have checked that a kinetic-energy cutoff of 340 eV for the plane-wave basis set and a charge-density cutoff of eight times larger are sufficient for the convergence of the total energy. Because of the large number of atoms per supercell we used only a single gamma point. For the calculation of the Fermi level we used Methfessel-Paxton method[23] with a smearing of 0.1 eV.

It is interesting to mention that we found that the electronic properties are not very sensitive to whether the LDA or the GGA+vdW exchange and correlation functionals are used. This seems surprising at first sight, however it is well known that LDA overbinds and GGA under binds. For example, LDA reproduces the distance between graphite layers[24] whereas GGA produces correct results only when the vdW interactions are included.[25] This seems also the case for our LDA and GGA+vdW calculations as it will be shown later. Beside the graphite results, the other reasons which motivated us to mainly present the LDA results are that (1) Ref. 26 found that for other molecules on metallic substrates the LDA distances are in better agreement with experiment and (2) Ref. 11 has shown that for MnPc and CuPc molecules, the experimental photoemission results agree with the LDA results. The Kohn-Sham self-consistent total energy is converged to within 10^{-6} Ry. For the atomic relaxation, the three lowest layers of copper are fixed whereas both the CoPc molecule and the topmost two metallic layers are fully relaxed. The force on the atoms are converged within 5×10^{-3} Ry/Å. To make sure our parameters and settings are reasonable, we checked that the density of states of the free CoPc molecule is in good agreement with existing results.[6]

III. RESULTS AND DISCUSSION

A. Stability of the CoPc molecule on Co(111) or Cu(111) substrates

For both Co(111) and Cu(111) substrates we have checked the three high-symmetry positions, i.e., the top position where the Co of the CoPc molecule is on top of a substrate atom, the bridge, and the hollow positions (see Fig. 1). We found that the bridge position are favored by CoPc molecule on both Co(111) and Cu(111) substrates. Notice that we have not differentiated between the hollow hcp and fcc positions,

TABLE I. Calculated LDA relative energy (eV) of CoPc molecule on different high-symmetry positions of the Co(111) and Cu(111) substrates (see Fig. 1). The value between parenthesis is obtained using the SIESTA code within the LDA (Ref. 27). The energy for the most stable position is set to zero.

Configurations	Bridge	Hollow	Top
CoPc/Co(111) (5 layers)	0	0.64 (0.67)	5.08
CoPc/Co(111) (3 layers)	0	0.62	5.05
CoPc/Cu(111) (5 layers)	0	0.31	1.28
CoPc/Cu(111) (3 layers)	0	0.31	1.30

and due to our limited computational power, we did not rotate the molecule with respect to the substrate to find its optimal position.

The relative energies for CoPc on different sites (the hollow, the bridge, and the top positions as shown in Fig. 1) are given in Table I. The calculated optimal distance between the molecule and the Co substrate is about 2.05 Å while it is about 2.39 Å for the Cu substrate. This suggests that the CoPc has stronger interaction with the Co(111) substrate. The LDA adsorption energy as a function of the distance between the molecule and the substrate is shown in Fig. 2(a). This curve is deeper for Co substrate, meaning that it will be harder to move the CoPc molecule on the Co substrate than on the Cu one. The magnetization of the Co atom within CoPc as a function of the distance between the molecule and the substrates is also shown in Fig. 2(b) and will be discussed later. Besides using the LDA, we also did calculations using the GGA+vdW method where the vdW dispersive forces are obtained within the Grimme approximation.[22] The results of the adsorption energies and magnetic moments are given, respectively, in Figs. 2(c) and 2(d). The distance between molecule and Co substrate calculated within the GGA+vdW is about 2.23 Å while it is about 2.70 Å between molecule and Cu substrate. It is not surprising that the GGA+vdW gives larger distances than LDA. This is because the GGA is known to overestimate distances. In fact the GGA alone produced distances of 2.70 Å and 3.4 Å for CoPc/Co(111) and CoPc/Cu(111), respectively, and the vdW dispersive forces reduced substantially these distances. However both LDA and GGA+vdW show that the distance between the molecule and Co substrate is smaller than the distance between molecule and Cu substrate, suggesting that the former one is a strong chemisorption while the latter one is a weak chemisorption at the limit of physisorption.

When a molecule is adsorbed on a metallic substrate, the electron-electron interactions will cause the rearrangements in the electronic structure of both components. To investigate the strength of these interactions we need to relax the struc-

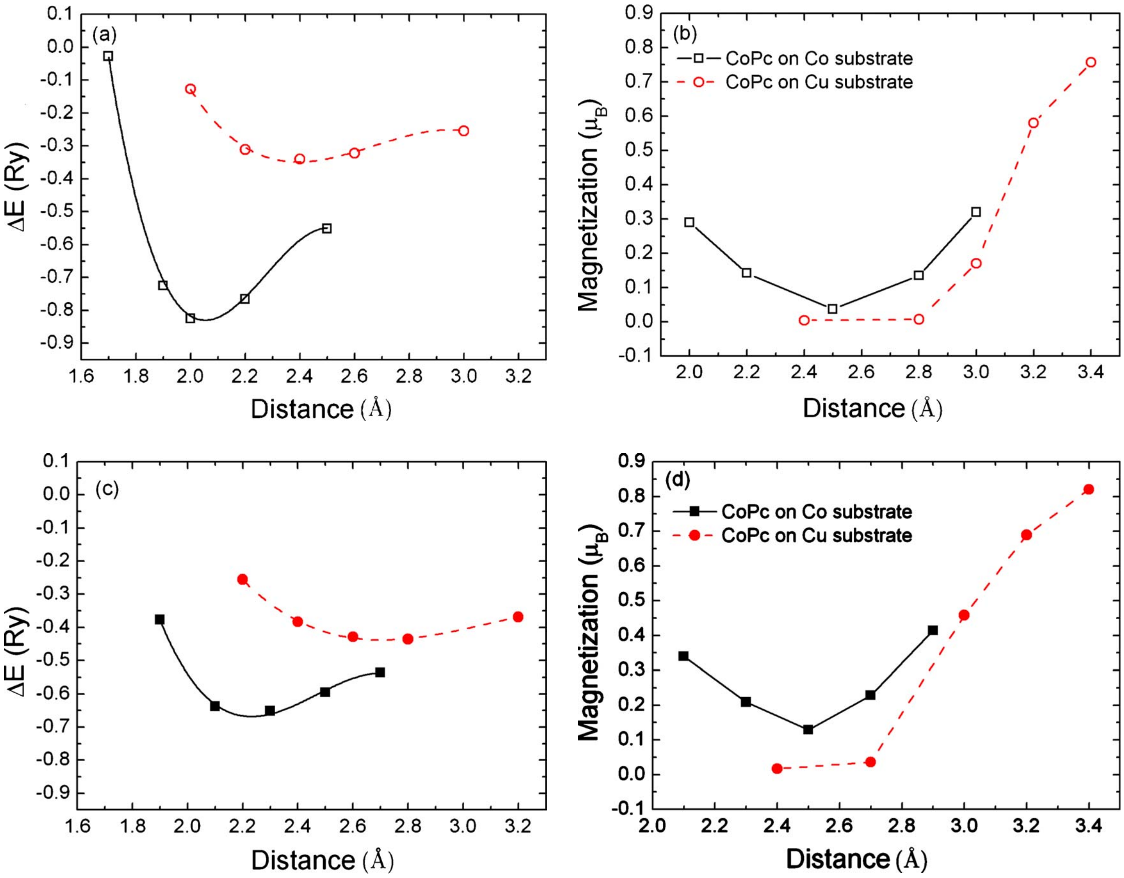

FIG. 2. (Color online) Calculated LDA (a) total energy Δ*E* and (b) magnetization of Co within CoPc compared to GGA+vdW, (c) total energy Δ*E* and (d) magnetization as a function of the distance between CoPc and Co(111) or Cu(111) substrates. The CoPc lay flat with respect to the surface. The magnetic moment of CoPc vanishes when the molecule gets closer to the Cu(111) substrate but develops only a minimum in the case of Co(111) substrate.

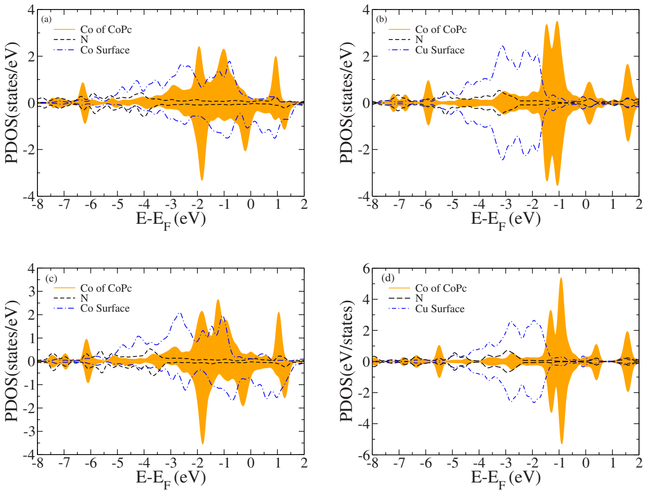

FIG. 3. (Color online) Calculated spin-polarized PDOS of various atoms of CoPc on (a) Co(111) substrate, using LDA, (b) Cu(111) substrate, using LDA, (c) Co(111) substrate, using GGA +vdW, and (d) Cu(111) substrate, using GGA+vdW (the spin up and spin down are shown, respectively, on the positive and negative vertical scales).

ture. It is found that, for both Co and Cu substrates, the CoPc molecule remain almost flat with respect to the surface. The maximum distortion toward the substrate occurs for the benzene rings and is lesser than 0.12 Å. It has a negligible effect on the electronic structure of the molecule and may be ignored, i.e., no significant change in the density of states is observed. The negligible distortions suggest that the influence of the Co or Cu substrates on the molecule are mainly produced by adjusting the molecule-substrate distance. The substrate has no preferential strong interaction with a particular atom of the molecule because if it were the case the CoPc molecule will have been strongly deformed.

B. Electronic and magnetic properties of CoPc molecule on Co(111) or Cu(111) substrates

The different effects of the two substrates can be seen from the density of states of the various atoms of the CoPc molecule and the substrate. Figure 3(a) shows the PDOS of the Co atom of the molecule, those of the N atoms, and the surface Co atoms, while Fig. 3(b) shows the same PDOS as Fig. 3(a) but for CoPc on Cu(111). A hybridization between the Co surface atoms and N atoms at binding energies between -5 and -4 eV and between Co atom of CoPc with the Co(111) surface at energies around -1 eV provide the chemical bonding of the molecule on the magnetic surface while only a smaller hybridization between Cu and CoPc at energies between -3 and -1 eV can be found for the paramagnetic Cu(111) surface. This means that the former is strongly chemisorbed while the latter is only weakly chemisorbed. From the PDOS of Co atom of CoPc, we find that the Co atom has a small magnetization when it is adsorbed on Co substrate but no magnetization when adsorbed on Cu substrate. In fact, the magnetization of Co of CoPc on the Co surface is 0.37 μ_B and is reduced from its calculated isolated molecule magnetization of 1.0 μ_B where the Co atom is a Co^{+2}. Some of N and C atoms have antiparallel or parallel induced spin magnetic moments with respect to the middle Co atom but all of them are lesser than 0.06 μ_B/atom. The magnetic moment of the Co surface layer also has changed from its pristine value of 1.77 μ_B/atom. When the CoPc is deposited on Co substrate the four atoms closest to the central Co atom of the molecule and located just below the first four nitrogen square have their magnetic moment reduced on average to 1.6 μ_B. The next square of Co atoms located below the next nitrogen square of the molecule have their moment reduced to 1.55 μ_B. Finally, the Co atoms forming a triangle below the benzene ring are reduced on average to 1.4 μ_B and those forming a diamond below the other benzene rings have magnetic moment of 1.38 μ_B along the vertical direction and 1.5 μ_B along the horizontal direction (see Figs. 1 and 5). Consequently, the CoPc molecule produces a magnetic pattern on the Co substrate which has the same shape as the molecule. It will be interesting to find a way to measure this magnetic print. The PDOS calculated using GGA+vdW are given in Fig. 3(c), where CoPc is on the Co substrate and in Fig. 3(d), where CoPc is on the Co substrate. For the Co substrate, LDA and GGA+vdW results show very slight differences, while for the Cu substrate, a significant difference is only found for the Co atom within the CoPc, however, the positions of different orbitals are still similar to those obtained using LDA. From Fig. 3, we observe that the hybridization between the molecular states and the substrate states are not sensitive to the choice of LDA or GGA+vdW.

For the Cu substrate, the magnetization of the Co of CoPc is destroyed by the influence of the paramagnetic surface. The substrate 4*s* electrons magnetically screen the spin of Co atom of CoPc. Like in the Kondo physics, the interaction between the localized spin of Co and the itinerant spins of the substrate results on a zero spin state. The dynamics of the mechanism cannot of course be captured by a band-structure calculation. All that density-functional calculation produces is a rearrangement of the *d* electrons of Co and 4*s* electrons of the substrate resulting in a Co net-zero-spin moment and a minimum total energy of the system.

From our calculation, we can deduce that the spin-polarized tunneling conductance can be obtained only when the CoPc molecule is deposited on a Co ferromagnetic surface but not for a Cu paramagnetic. We will return to this point later when we compute the electric conductance.

The calculated PDOS per orbital of Co atom in the molecule is shown in Fig. 4. Notice that LDA and GGA+vdW produce very similar DOS. Because of the electronic interactions and charge transfer between the substrate and the molecule, the energy position of the molecular orbitals are shifted with respect to each others. For the Co substrate, the d_{zx} and d_{zy} orbitals are no longer degenerate which is caused by the strong interaction between the molecule and the hcp Co surface which is asymmetrical along the x and y directions (see Fig. 1). When the molecule is on the paramagnetic surface (Cu), all the orbitals have the same density states for spin-up and spin-down electrons resulting in a zero spin magnetic moment on the Co site of CoPc. Because of the weaker interaction of the molecule and the surface, the DOS of d_{zx} and d_{zy} orbitals are almost identical even though the

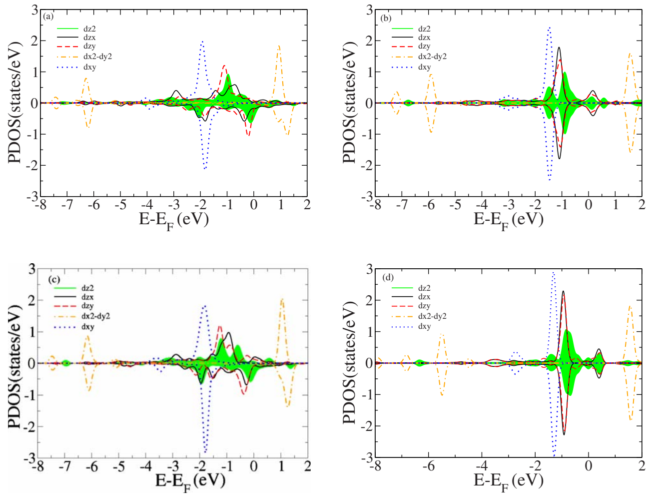

FIG. 4. (Color online) Calculated PDOS of 3*d* orbitals of Co in CoPc (in terms of cubic harmonics) adsorbed on (a) Co(111) substrates, using LDA, (b) Cu(111) substrates, using LDA, (c) Co(111) substrates, using GGA+vdW, and (d) Cu(111) substrates, using GGA+vdW. The spin up and spin down are shown, respectively, on the positive vertical and negative scales.

Cu(111) surface is asymmetric. It is interesting to notice that in both cases, only the d_{zx}, d_{zy}, and d_{z^2} are present at the vicinity of the Fermi level since they are the only orbitals that interact with the substrate.

From the above calculations, it can be concluded that both Co(111) and Cu(111) substrates reduce drastically the magnetization of the CoPc molecule. In order to understand the mechanism behind this effect, the magnetization of the Co within CoPc, the total molecular spin-polarized DOS (MDOS) and the magnetic structure of the CoPc on Co and Cu substrates are calculated for different distances between the flat-lying molecule and each of the Co and Cu substrates. To make the figure readable, the magnetic structures shown in Fig. 5 are the differences between the magnetization of the molecule on the substrate and the free substrate. For the CoPc on Cu substrate, the magnetization of molecule decreases with the decreasing distance as shown in Fig. 2(b). That is because when the distance decreases, the charge transfer increases causing the energy states of the molecule to shift and allowing the 4*s* substrate electrons to efficiently magnetically screen the Co spin moment. If we compare the MDOS of CoPc on Cu substrate in Figs. 5(d)–5(f) with the MDOS of free CoPc molecule [see the inset in Fig. 5(c)] it can be clearly seen that the energy states of the spin-down

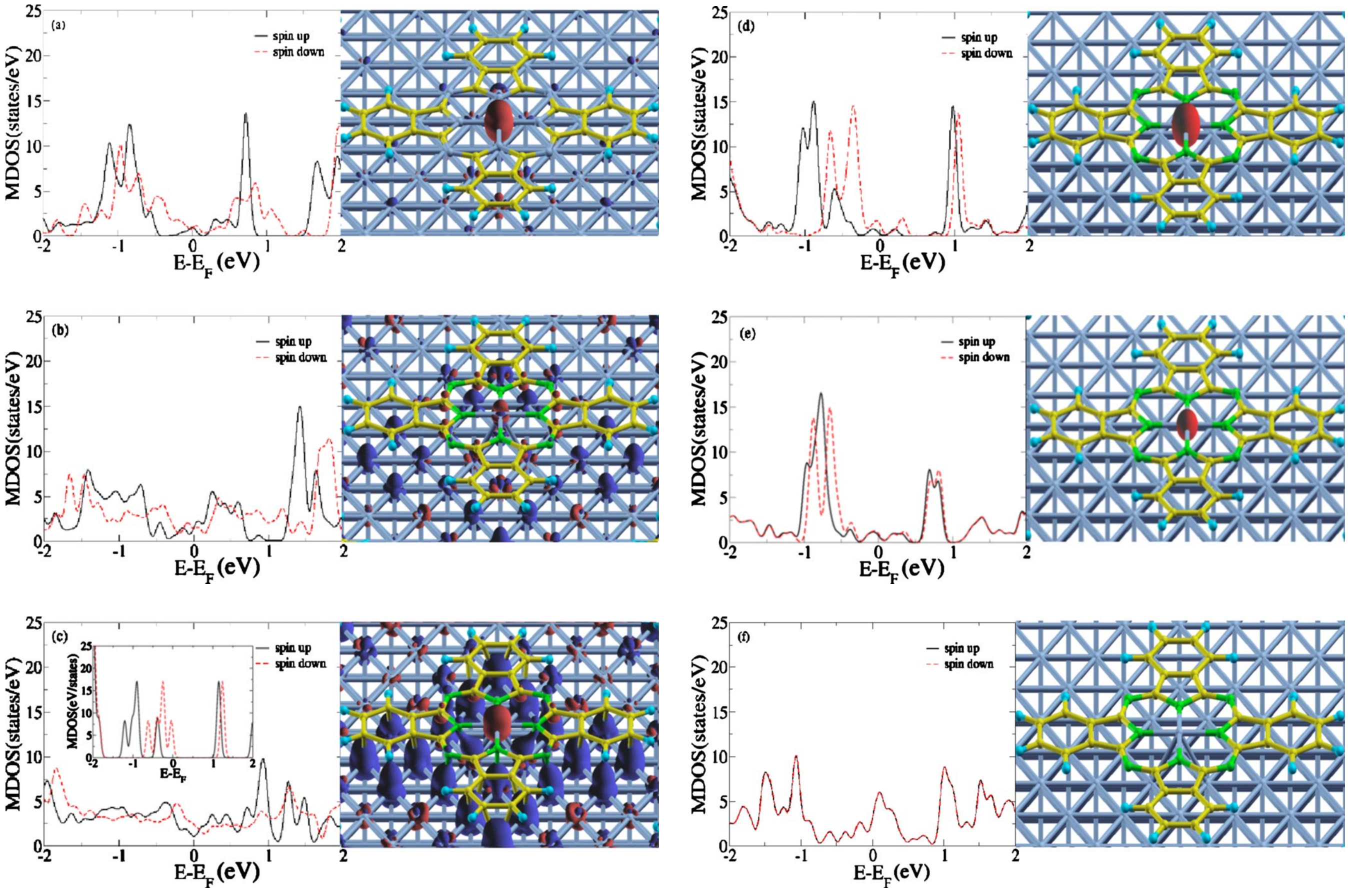

FIG. 5. (Color online) Calculated total spin-polarized molecular density of states (MDOS) (full line spin up and dashed line spin down) and isosurface of the difference of magnetizations (see text), where red (dark gray) is spin up and blue (light gray) is spin down, of CoPc on Co substrate when the distance between the substrate and the molecule is (a) 3.0 Å, (b) 2.5 Å, and (c) 2.0 Å (in the inset, the DOS of the free CoPc molecule shows an energy gap of 1 eV between the LUMO and HOMO and a magnetic moment of 1 μ_B) and on Cu substrate when the distance is (d) 3.4 Å, (e) 3.0 Å, and (f) 2.4 Å.

TABLE II. Calculated charge difference between CoPc molecule on Co(111) or Cu(111) substrates.

		$Co_\uparrow$	$Co_\downarrow$	Co	N	C	Molecule
LDA	CoPc/Co(111)	−0.2381	0.4589	0.2209	0.1608	0.0818	4.1921
	CoPc/Cu(111)	−0.3720	0.6164	0.2444	0.0334	0.0605	2.4300
GGA+vdW	CoPc/Co(111)	−0.2462	0.5060	0.2598	0.0441	0.0771	3.0493
	CoPc/Cu(111)	−0.3592	0.6324	0.2732	0.0410	0.0020	1.6359

electrons shift toward lower energies and at the equilibrium distance they become the same as the energy states of spin-up electrons [notice that for the free molecule, the band gap between lowest-unoccupied molecular orbital (LUMO) and the highest-occupied molecular orbital (HOMO) is about 1 eV]. This makes the molecule lose its magnetization when its deposited on the Cu substrate. The situation is more complex for the Co substrate. The magnetization of the Co atom of CoPc first decreases and then increases with the decreasing distance. From Figs. 5(a)–5(c), it can be seen that when the molecule is far from the Co substrate only the Co of CoPc has a magnetization. However, as the distance continually decreases, some new magnetic states appear. The N and C atoms near the Co atom within CoPc become polarized, the N atoms have antiparallel magnetic moments while C atoms have parallel magnetic moments. When the molecule reaches the equilibrium distance, some C atoms far from Co atom within CoPc become slightly magnetized because of the large interaction between the CoPc and Co substrate. From the MDOS of CoPc on Co substrate, it can be found that the energy states of CoPc molecule and Co substrate are strongly mixed. Even when the CoPc is far from the Co substrate. This change in MDOS is pronounced especially for the spin-down electrons. It is interesting to notice that when CoPc is at 2.5 Å from Co substrate and 2.4 Å from Cu substrate, the magnetization of Co atom of CoPc vanishes in both cases, but the magnetic states are totally different. The latter one is much more complex. The increase in the magnetic moment of Co in CoPc on Co(111) could be due to a competition between the exchange interaction and charge transfer between the first layer of Co substrate and the molecule. This is because at such distances a strong hybridization occurs between the 3*d* orbitals of Co whereas this not the case for the Cu substrate since the *d* orbitals are completely filled.

C. Charge transfer and electric dipole at the interface

The charge transfer at the interface has a crucial influence on the magnetization of CoPc and it is calculated using Löwdin orthogonalization and population analysis.[28] Table II shows the results of the charge transfer per atom of CoPc and the whole molecule. From the table we notice that the charge transfer occurs from the substrate to the molecule for both Co and Cu substrates. As the distance from the CoPc molecule to the Co substrate is much shorter than the distance from the CoPc to the Cu substrate, it results more charge transfer from the Co substrate to the CoPc molecule. For the electrons of Co atom of CoPc, the spin-up electron population decreases, while that of spin-down increases. This reduces drastically the magnetization of CoPc. In the case of CoPc on Cu(111) substrate the magnetization of CoPc vanishes because of the absence of exchange field. Indeed the 3*d* orbitals of Cu are filled and only the 4*s* electrons interact with the molecule and screen the Co spin moment. In order to confirm that the observation of charge transfer and magnetization transfer is not an artifact due to the use of LDA functional, which may lead to the overdelocalization of the electronic density, we also presented the results from GGA +vdW calculations. They are in agreement with the LDA results, except the GGA+vdW charge transfer and magnetization transfer are somewhat less strong than those produced by means of the LDA. This is due to the fact that GGA +vdW calculations produced a slightly larger molecule-substrate distances when compared to the LDA ones. We have also calculated the charge transfer of CoPc on Co and Cu substrates for different molecule-substrate distances. It is found that the charge transfer of Co atom of CoPc increases almost linearly as the distance decreases while the spin transfer first deceases and then increases as the distance decreases for CoPc on Co(111) substrate. As a consequence the magnetization of the Co atom of CoPc has a minimum value for the molecule substrate of about 2.5 Å.

The rearrangement of the electrons at the interface and molecule-substrate interaction can be also described by the redistribution of the electron charge density in real space as shown in Fig. 6. The real-space charge redistribution, $\delta\rho(z)$ occurring due to the molecule-substrate interaction is calculated in the following manner:

$$\delta\rho(z) = \rho_{mol+sub}(z) - [\rho_{mol}(z) + \rho_{sub}(z)], \tag{1}$$

where $\rho_{mol+sub}(z)$ is the electron density of the combined system while $\rho_{mol}(z)$ and $\rho_{sub}(z)$ are the electron densities of the noninteracting molecule and substrate, respectively. Those densities are integrated over the *x*-*y* plane within the unit cell. Figure 6(a) shows that the total and spin polarized $\delta\rho(z)$ oscillates, which is a typical behavior for a molecule-metal interface.[29–31] The charge rearrangement decays rapidly away in both sides of the metal-molecule interface. the strong electronic interaction of CoPc with the Co(111) reduces the distance between the flat-lying CoPc molecule and the Co(111) and produces a much stronger rearrangement of the electron density than when CoPc is deposited on Cu(111) substrate. As a consequence a substantial loss of the electron density above the topmost Co layer and therefore a strong gain of the electron density right below the topmost Co layer has been found. It is interesting to notice that the charge

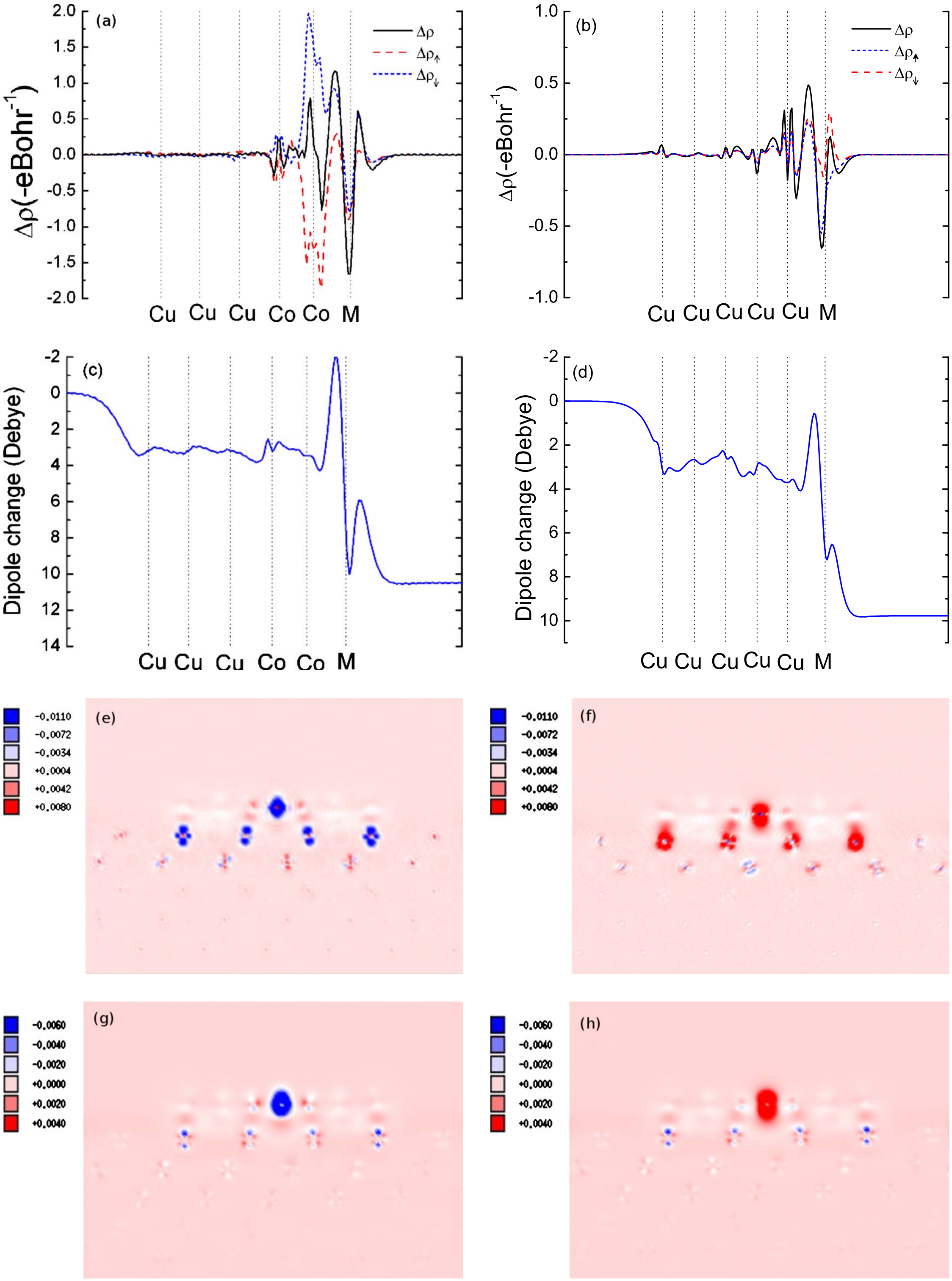

FIG. 6. (Color online) Calculated LDA $\delta\rho(z)$ of CoPc on (a) Co(111) and (b) Cu(111) substrates, dipole moment change $\delta\mu(z)$ of CoPc on (c) Co(111) and (d) Cu(111) substrates, and spin-polarized charge-density differences $\delta\rho_\sigma(\mathbf{r})$ for (e) spin up and for (f) spin down of CoPc on Co substrate, and (g) spin up and (h) spin down of CoPc on Cu(111) substrate. The red (light-gray) region is where the charge is accumulated and the blue (dark-gray) one is where the charge is depleted.

density of the atoms of Co below the molecules lose electrons and those of spin-down gain electrons which explain the reduction in the surface Co atoms laying below the CoPC molecule. On the molecule side, the electron density in the plane of the CoPc atoms is depleted while the region above and below the plane gain electrons. This behavior is due to the interaction of the CoPc with the substrate making the π bonding gain electrons and the in-plane σ bonding lose electrons. The situation is similar in the case of CoPc on Cu(111) substrate but less pronounced.

The dipole moment change ($\delta\mu$) induced by adsorption shown in Fig. 6(b) is given by

$$\delta\mu = -\int_{z_b}^{z_b+a} (z - z_0)\,\delta\rho(z)dz, \tag{2}$$

where z_b is the center of vacuum region, z_0 is the top surface layer, and a us the length of the unit cell in the z direction. Note that a positive (negative) value indicates a dipole oriented to the vacuum (substrate) side.

The adsorption-induced dipole moment change $\delta\mu$ and the change in work function $\delta\psi$ are related by Helmholtz equation, which in atomic units reads[32]

$$\delta\psi = -4\pi\theta\delta\mu, \tag{3}$$

where $\delta\psi$ is in hartree, $\delta\mu$ is the dipole moment change per unit cell in units of electron bohr, and θ is an absolute converge in the units of bohr^{-2} (i.e., $\theta = \theta/a_0$, where θ is a fractional coverage and a_0 is the area of the surface unit cell). Since the θ is about 0.45 in our case, the LDA $\delta\psi$ calculated by the above equation are −0.88 eV and −0.82 eV for CoPc on Co and Cu substrates, respectively. In the other hand the work function is defined by the difference between the electrostatic potential energy in the vacuum and the Fermi energy and is found to be 5.14 eV for both bare Co and Cu substrates. This work function becomes 4.23 eV for CoPc on Co substrate and 4.32 eV for the CoPc on Cu substrate, leading to a $\delta\psi$ of −0.91 eV and −0.82 eV for the CoPc on Co and Cu substrates, respectively. The two results are in excellent agreement with the results obtained from the surface dipole. Several origins can be responsible for the change in work function such as: (1) charge transfer, (2) chemical interaction, (3) push back effect due to Pauli repulsion between metal and molecular electrons. Considering that the chemical interaction is only significant for CoPc on Co substrate and the charge transfer is from substrates to the molecule which will increase the work function. The reduction in the work function for Cu and Co substrate is mainly caused by the push back effect which is a purely quantum effect.[33,34]

Figures 6(e)–6(h) show LDA $\delta\rho_{\uparrow}(\mathbf{r})$ and $\delta\rho_{\downarrow}(\mathbf{r})$ in the plane perpendicular to the substrate and passing through the Co and the first-neighbor nitrogen atoms of CoPc. Again, we observe the rearrangement of the electron density is more pronounced for the molecule on the Co substrate. For the Co substrate, the electron-density rearrangement occurs between the molecule and the top two Co layers, while for the Cu substrate, the electron-density arrangement occurs almost only between the molecule and the topmost Cu layer. The rearrangement of electron density occurs in a complex way but is similar to Friedel electron oscillations at the vicinity of an impurity atom in a metal. It is interesting to notice that Co atom of CoPc on Co substrate exhibits a spin-flip effect, i.e., its spin-up electron charge density is depleted while those for the spin down are enhanced. No spin-flip effects are found for the CoPc on Cu substrate. In addition, from Figs. 6(e) and 6(g), we can clearly see the charge density accumulates between the CoPc molecule and Co substrate atoms while it depletes between the atoms of the molecule which means that some bonds of the molecule are weakened and new bonds are created between molecule and the substrate.

D. STM images and transport properties

The STM images of both CoPc/Co(111) and CoPc/Cu(111) have been calculated using Tersoff-Hamann approximation.[13] Considering the experimental data [see Figs. 5(c)–5(f) of Ref. 5], we calculated the STM of CoPc on the Co substrate at potential biases of −0.2 and 0.9 eV with respect to the Fermi level, and that of CoPC on the Cu substrate at the biases of −0.7 and 0.4 eV. The results are given in Fig. 7. We observe that the STM images of the CoPc/Co are somewhat similar to those of CoPc/Cu. At first hand, this looks like the two systems have similar molecular orbitals for the chosen energies in qualitative agreement with the features observed experimentally.[5] This suggest that, as observed by the authors of Ref. 5, the maximum of the DOS of the molecule in the two systems is shifted by about 0.5 eV from each other. We do not fully agree with this statement since the molecular DOS, as shown in Fig. 3, do not only exhibit a simple energy shift. In fact the DOS of Co in CoPc when adsorbed on Co(111) has an exchange splitting on the order of 1 eV at the Fermi level and is more metalliclike whereas that of Co over Cu(111) has no exchange splitting and looks more molecularlike.

In fact, the energy shift of about 500 meV can be explained qualitatively by the fact that the adsorption of the CoPC molecule on Co(111) is much stronger than that on Cu(111). This leads to a much larger charge transfer from the Co substrate to the molecule (see Table II). This huge charge transfer in the case CoPc/Co(111) pins the HOMO to the Fermi level. From the STM images we can directly observe the different adsorption mechanisms of the nonmagnetic and magnetic substrates. The STM image of the molecule on the Cu surface, at 0.4 eV bias, shows the symmetry of the free molecule while that of CoPc/Co, at 0.9 eV bias, shows a much complicated symmetry. The strong chemical bonds between the Co substrate and the molecule break the original symmetry of the molecule. This is compatible with the fact that the former one exhibits a weak chemisorption and the latter one a strong chemisorption.

We have also investigated the spin-polarized scanning tunneling properties of CoPc on Co(111) substrate. For the tip, we used the model of Co(111) surface consisting of a (4×4) supercell with five layers plus 11 Co atom pyramid cluster adsorbed on these layers. The structure is shown in Fig. 8(a) and the PDOS of the top Co atom is given in Fig. 8(b). When the interaction of the tip and the sample can be neglected, the STM I-V curves of the tip on the Co atom within the Pc molecule can be calculated by means of the modified Bardeen approximation,[10,14]

$$I = \frac{4\pi e}{\hbar}\int_{E_F}^{E_F+eV} \rho_s(E)\rho_t(E-eV)|M_{st}|^2 dE, \tag{4}$$

where E_F is the Fermi level, V is the bias voltage added to the STM tip, ρ_s, ρ_t are the DOS of the Co atom within CoPc and topmost atom of Co tip, and M_{st} are the tunneling matrix

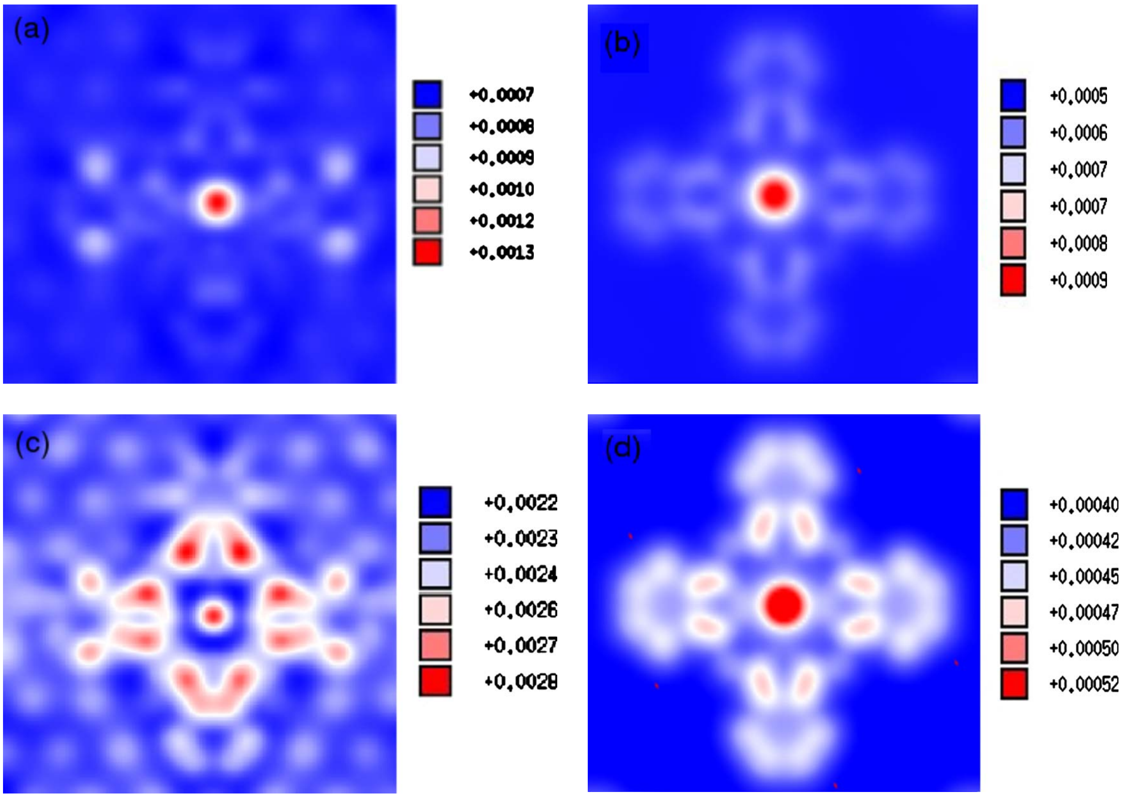

FIG. 7. (Color online) [(a) and (c)] STM images of CoPc on Co substrate at biases of −0.2 eV and 0.9 eV, respectively. [(b) and (d)] STM images of CoPc on Cu(111) substrate at the bias of −0.7 eV and 0.4 eV, respectively.

elements. Since the *d* states dominate the DOS at the Fermi level for both Co atom within CoPc on Co substrate and the top Co atom of the tip and since the tip is placed on top of the Co of CoPc, we consider therefore only the tunneling of the electrons emanating from the Co *d* orbitals. It was shown that the electron tunneling probability between orbitals of

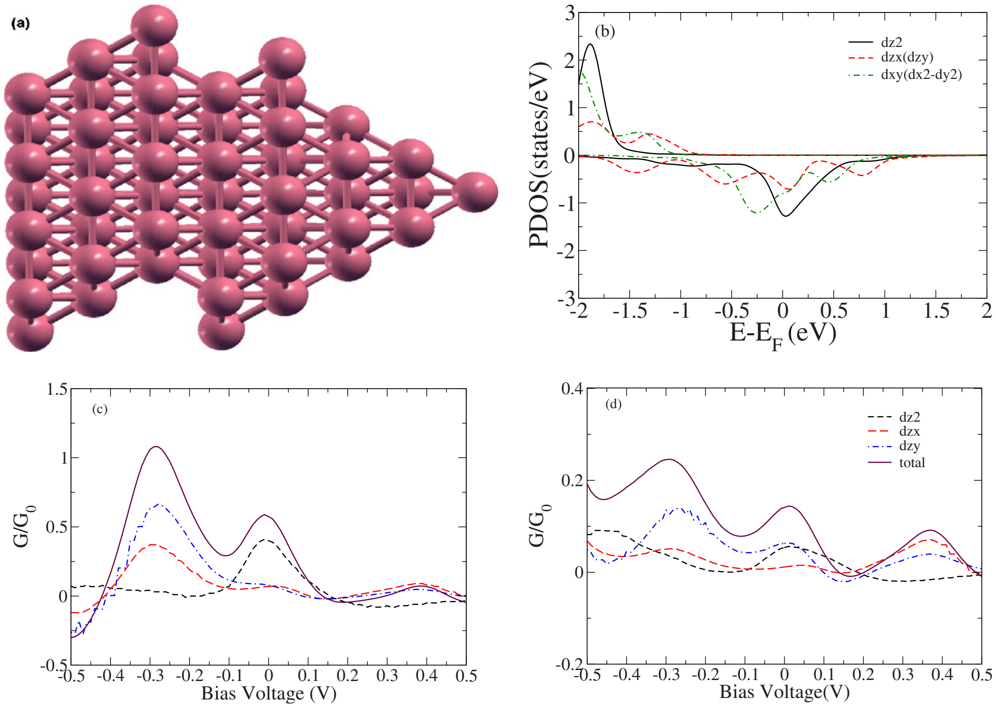

FIG. 8. (Color online) (a) The structure of tip used in the calculation of the *I*-*V* characteristics. (b) The PDOS of the top Co atom of the tip decomposed into different types of *d* spin-polarized orbitals. (c) and (d) represent the normalized conductance for parallel and antiparallel magnetizations and decomposed into various cubic symmetries of the *d* orbitals.

different magnetic numbers is extremely small in comparison to those between orbitals of same magnetic number.[10] This is essentially caused by the spatial-symmetry mismatching. In addition, we assume that the tunneling rates between the sample and tip for the d_{z^2}, d_{zx}, d_{zy}, $d_{x^2-y^2}$, and d_{xy} orbitals are the same. The above equation can be therefore further simplified to

$$I = C\int_{E_F}^{E_F+eV} \sum_m \rho_s^m(E)\rho_t^m(E-eV)dE, \qquad (5)$$

where C is the constant depends on the distance between the tip and sample and m is the magnetic number of the d orbitals. The modified differential conductances G/G_0 (where $G = dI/dV$ and G_0 is a constant) are given in Fig. 8(c) when the magnetization of the tip is parallel to that of the Co substrate and in Fig. 8(d) for the antiparallel case. From the model calculation, we can find that d_{z^2}, d_{zx}, and d_{zy} orbital are responsible for the tunneling of the electrons in the low bias and that a large magnetoresistance effect is obtained. For both parallel and antiparallel cases, we found a strong peak at about −0.3 V bias corresponding to large PDOS peak of d_{zx}, d_{zy} symmetry (see Fig. 4) and a small peak at 0 V bias corresponding to the Co in CoPc d_{z^2} PDOS symmetry. The peak around 0 V is due mainly to the alignment of the maximum PDOS of d_{z^2} orbital of the STM tip with a weaker one due to Co in CoPc. It will therefore strongly depend on the choice of the STM tip because for another type of STM tip the d_{z^2} PDOS peak will not be necessary at the Fermi level and will not therefore align with the d_{z^2} peak of PDOS of Co in CoPc at zero bias. However the peak at about −0.3 V is caused by a strong maximum PDOS of d_{zx}, d_{zy} symmetry of the Co atom in CoPc, and will be less affected by the electronic structure of the STM tip. This latter peak in the conductance compares qualitatively with the experimental peak observed at −0.2 V using a Co-coated tip.[9] Indeed the calculated magnetoresistance ratio $(G_P - G_{AP})/(G_P + G_{AP})$ for a bias of −0.3 eV is 0.63 and is about three times larger than the observed peak.[9] However, the theory shows a ratio of 0.61 at zero bias not observed in experiment.[9] We believe that the transport properties obtained using STM depend strongly on the nature of the tip. As shown in Fig. 8 the Co tip has large DOS at the Fermi level which is essential in getting the peak in the conductance (as shown in Fig. 8). The comparison with experiment remains only qualitative since the simplified Bardeen approximation is crude. A more sophisticated calculation of the STM transport within the nonequilibrium Green's function and based on our electronic calculation will certainly produce more accurate results than the Bardeen approximation.

IV. CONCLUSION

We have used a plane-wave *ab initio* ultrasoft pseudopotential method within both the LDA and GGA+vdW functionals to investigate the effects of a paramagnetic or ferromagnetic substrate on the electronic structure, the magnetism, and electronic transport properties of CoPc molecule. We have found that the equilibrium molecule-substrate distance is smaller for a Co(111) ferromagnetic substrate as compared to a paramagnetic Cu(111) substrate. This difference in distance was the result of stronger electronic interactions between the CoPc and the d electrons of Co substrate. For both the Co(111) and Cu(111) substrate we showed that CoPc molecule prefers the bridge position. The density of states, the charge transfer, and the STM of the molecule on the two substrates have been calculated. All the results show that the molecule is strongly chemisorbed on Co surface while it is weakly chemisorbed on the Cu surface. We have also explained the magnetic state of the Co atom of the Pc molecule based on the charge transfer and bonding of the Co d orbitals to the Co(111) or the Cu(111) substrates. In particular, the charge transfer from the substrate to the molecule suppresses completely the magnetic moment of CoPc on Cu(111) and reduced it strongly for the CoPc on Co(111). This substrate s orbital screening of the CoPc magnetic moment is similar to a Kondo-type physics and is a pure theoretical prediction that we hope will be checked experimentally in the near future. We have also shown that the interaction of the CoPc with the substrate reduces significantly the surface work function that also can be checked experimentally.

Our calculation of STM images within the Tersoff-Hamann approximation[13] confirmed the energy shift observed experimentally for STM images of CoPc on Co(111) and Cu(111). Finally we calculated the STM spin-polarized conductance for CoPc on Co(111) within the modified Bardeen approximation[14] where the STM tip was modeled by a Co pyramid cluster on top of few monolayers of Co. The results were only in qualitative agreement with the experimental results.[9] We believe that a much sophisticated STM transport calculation within the nonequilibrium Green's function based on our results will produce a much better agreement with experiment. We are optimistic however that our calculation will be helpful for the understanding of future experimental results and might be useful for describing the physics of CoPc molecular junctions.

ACKNOWLEDGMENTS

We acknowledge support from an ANR pnano under Grant No. ANR-06-NANO-053-01. This work was performed using HPC resources from GENSI-CINES under Grant No. 2009-gem1100. We would like to thank E. Beaurepaire and his experimental group for useful discussions about the experimental STM images.

[1] C. Joachim, J. K. Gimzewski, and A. Aviram, Nature (London) **408**, 541 (2000).

[2] A. Nitzan and M. A. Ratner, Science **300**, 1384 (2003).

[3] A. R. Rocha, V. M. García-suárez, S. W. Bailey, C. J. Lambert, J. Ferrer, and S. Sanvito, Nature Mater. **4**, 335 (2005).

[4] J. Reichert, R. Ochs, D. Beckmann, H. B. Weber, M. Mayor, and H. V. Löhneysen, Phys. Rev. Lett. **88**, 176804 (2002).

[5] A. F. Takács, F. Witt, S. Schmaus, T. Balashov, M. Bowen, E. Beaurepaire, and W. Wulfhekel, Phys. Rev. B **78**, 233404 (2008).

[6] A. Zhao, Q. Li, L. Chen, H. Xiang, W. Wang, S. Pan, B. Wang, X. Xiao, J. Yang, J. G. Hou, and Q. Zhu, Science **309**, 1542 (2005).

[7] G. Chiappe and E. Louis, Phys. Rev. Lett. **97**, 076806 (2006).

[8] J. M. Aguiar-Hualde, G. Chiappe, E. Louis, and E. V. Anda, Phys. Rev. B **76**, 155427 (2007).

[9] C. Iacovita, M. V. Rastei, B. W. Heinrich, T. Brumme, J. Kortus, L. Limot, and J. P. Bucher, Phys. Rev. Lett. **101**, 116602 (2008).

[10] L. Chen, Z. Hu, A. Zhao, B. Wang, Y. Luo, J. Yang, and J. G. Hou, Phys. Rev. Lett. **99**, 146803 (2007).

[11] A. Calzolari, A. Ferretti, and M. B. Nardelli, Nanotechnology **18**, 424013 (2007).

[12] X. Chen, Y. S. Fu, S. H. Ji, T. Zhang, P. Cheng, X. C. Ma, X. L. Zou, W. H. Duan, J. F. Jia, and Q. K. Xue, Phys. Rev. Lett. **101**, 197208 (2008).

[13] J. Tersoff and D. R. Hamann, Phys. Rev. B **31**, 805 (1985).

[14] J. Bardeen, Phys. Rev. Lett. **6**, 57 (1961); see also C. J. Chen, *Introduction to Scanning Tunneling Microscopy* (Oxford University Press, Oxford, 1993).

[15] P. Giannozzi, S. Baroni, N. Bonini, M. Calandra, R. Car, C. Cavazzoni, D. Ceresoli, G. L. Chiarotti, M. Cococcioni, I. Dabo, A. Dal Corso, S. de Gironcoli, S. Fabris, G. Fratesi, R. Gebauer, U. Gerstmann, C. Gougoussis, A. Kokalj, M. Lazzeri, L. Martin-Samos, N. Marzari, F. Mauri, R. Mazzarello, S. Paolini, A. Pasquarello, L. Paulatto, C. Sbraccia, S. Scandolo, G. Sclauzero, A. P. Seitsonen, A. Smogunov, Paolo Umari, and R. M. Wentzcovitch, J. Phys.: Condens. Matter **21**, 395502 (2009).

[16] The LDA calculations were done using PWSCF QUANTUM ESPRESSO-4.0.5 package and the GGA+vdW was done by using ESPRESSO-4.2 package which includes the vdW Grimme implementation (Ref. 22). The calculation were performed on the CINES French computer facility, http://www.cines.fr, on a SGI Altix ICE supercomputer using Intel Quad-Core E5472 or X5560 with a 32 Gb memory per node. The operating system is a Linux 64 bits. The LAPACK and BLAS libraries are provided by the INTEL MKL LIBRARY.

[17] P. Hohenberg and W. Kohn, Phys. Rev. **136**, B864 (1964); W. Kohn and L. J. Sham, Phys. Rev. **140**, A1133 (1965).

[18] J. P. Perdew, K. Burke, and M. Ernzerhof, Phys. Rev. Lett. **77**, 3865 (1996).

[19] A. M. Rappe, K. M. Rabe, E. Kaxiras, and J. D. Joannopoulos, Phys. Rev. B **41**, 1227 (1990).

[20] http://www.pwscf.org

[21] J. P. Perdew and A. Zunger, Phys. Rev. B **23**, 5048 (1981).

[22] S. Grimme, J. Comput. Chem. **27**, 1787 (2006); for the PWSCF implementation see V. Barone, M. Casarin, D. Forrer, M. Pavone, M. Sambi, and A. Vittadini, *ibid.* **30**, 934 (2009).

[23] M. Methfessel and A. T. Paxton, Phys. Rev. B **40**, 3616 (1989).

[24] L. Spanu, S. Sorella, and G. Galli, Phys. Rev. Lett. **103**, 196401 (2009).

[25] H. Rydberg, M. Dion, N. Jacobson, E. Schroder, P. Hyldgaard, S. I. Simak, D. C. Langreth, and B. I. Lundqvist, Phys. Rev. Lett. **91**, 126402 (2003).

[26] L. Romaner, D. Nabok, P. Puschnig, E. Zojer, and C. Ambrosch-Draxl, New J. Phys. **11**, 053010 (2009).

[27] A. Jaafar and M. Alouani (unpublished); the calculation are done using the SIESTA code, see J. M. Soler, E. Artacho, J. D. Gale, A. Garca, J. Junquera, P. Ordejón, and D. Sánchez-Portal, J. Phys.: Condens. Matter **14**, 2745 (2002).

[28] P. O. Löwdin, J. Chem. Phys. **18**, 365 (1950); Adv. Phys. **5**, 1 (1966).

[29] G. Heimel, L. Romaner, J. L. Brédas, and E. Zojer, Phys. Rev. Lett. **96**, 196806 (2006).

[30] P. Sony, P. Puschnig, D. Nabok, and C. Ambrosch-Draxl, Phys. Rev. Lett. **99**, 176401 (2007).

[31] A. Alkauskas, A. Baratoff, and C. Bruder, Phys. Rev. B **73**, 165408 (2006).

[32] S. Peljhan and A. Kokalj, J. Phys. Chem. C **113**, 14363 (2009).

[33] P. S. Bagus, V. Staemmler, and C. Wöll, Phys. Rev. Lett. **89**, 096104 (2002).

[34] A. Michaelides, P. Hu, M.-H. Lee, A. Alavi, and D. A. King, Phys. Rev. Lett. **90**, 246103 (2003).